Biosensors and Bioelectronics 41 (2013) 649–655

Contents lists available at SciVerse ScienceDirect

Biosensors and Bioelectronics

journal homepage: www.elsevier.com/locate/bios

Dielectrophoretic responses of DNA and fluorophore in physiological solution by impedimetric characterization

Shanshan Li [a,b], Quan Yuan [a], Bashir I. Morshed [c], Changhong Ke [d], Jie Wu [a,*], Hongyuan Jiang [b]

[a] Department of Electrical Engineering and Computer Science, the University of Tennessee, Knoxville, TN 37996, USA
[b] School of Mechatronics Engineering, Harbin Institute of Technology, 150001, PR China
[c] Department of Electrical and Computer Engineering, University of Memphis, Memphis, TN 38152, USA
[d] Department of Mechanical Engineering, State University of New York at Binghamton, Binghamton, NY 13902, USA

ARTICLE INFO

Article history:
Received 11 August 2012
Received in revised form
17 September 2012
Accepted 21 September 2012
Available online 28 September 2012

Keywords:
AC electrokinetics
Dielectrophoresis
DNA
Impedimetric detection

ABSTRACT

Characterization of the DNA's dielectrophoretic (DEP) behavior is the foundation of DNA manipulation by electric fields. This paper presents a label-free DNA differentiation technique by a combination of DEP response and impedimetric measurement on the microchip.

In contrast to most of the recent studies on DEP manipulation of DNA that use deionized water or diluted DNA buffer where living biomolecules cannot survive, we used physiological solutions (PBS with 154 mM Na+) that are highly practical for pursuing DNA-based physical applications. The microchip, a commercial surface acoustic wave resonator, contains an array of interdigitated aluminum electrodes (1.4 μm width, 1.1 μm gap) on quartz substrate for DEP trap. Measurements were taken with a high precision impedance analyzer, which also acted as the excitation source to induce DEP response at 20 kHz, 50 kHz, 100 kHz, 300 kHz, 500 kHz, 1 MHz, 2 MHz and 5 MHz ($N=3$). To verify DEP response, fluorescence microscope images were captured before and after the electric excitation. Test results from the DEP experimentation after comparing with fluorescent images of pUC18 DNA show that a large change in impedance corresponds to positive DEP while little change corresponds to negative DEP. The strongest *p*-DEP and the maximum collection efficiency were observed around 300 kHz for supercoiled pUC18 and 100 kHz for linear λDNA. This work yields real-time impedimetric DEP response of DNA of different molecular conformations in practical settings. The technique can serve as the basis for submicron particle separation, disease diagnosis, cell life-circle research, and other applications in physiological surroundings.

1. Introduction

Deoxyribonucleic acid (DNA) separation has numerous applications in fundamental DNA research, biotechnology and medicines. Though significant progress has been made, the existing DNA separation techniques are mostly based on electrophoresis techniques, in which the separation of DNA is conducted in bulk quantity and in a slow fashion and requiring very high working voltage (Kheterpal and Mathies, 1999). Rapid and single-molecule level DNA separation techniques, for which there is a pressing need in the area of single molecule level DNA research and to develop DNA-based physical applications (e.g. radiation sensors and Nano robots), are still not available.

The work here presents rapid label-free differentiation of DNA by combining impedimetric measurement with dielectrophoresis (DEP) concentration. The study of impedance spectroscopy could date back to 1975 (Lorenz and Schulze, 1975). However, employing microelectrodes in impedance sensing is still in a developing stage, and microelectrode impedimetric sensing is a very active research area. Because of their small characteristic dimension, microelectrodes are well suited for sensing the formation of protein complexes or assembly of protein arrays at electrode surfaces and for characterizing the process of material deposition. The underlying mechanism is that material changes near the electrode surface will cause changes in the impedance between the microelectrodes, thus providing a direct means of detecting binding reactions on the electrode surfaces Wang et al., 2004. The impedance response is generally proportional to the amount of bounded macromolecules, thus can potentially be used for quantitative measurements. Another advantage of impedimetric sensing is that it does not require molecular labeling, which simplifies the sample preparation and reduces the number of steps in the assay workflow. Presently, research efforts in the area of microelectrode impedimetric sensing are focused on expanding

* Corresponding author. Tel.: +1 865 974 5494; fax: +1 865 974 5483.
E-mail address: jaynewu@utk.edu (J. Wu).

0956-5663/$ - see front matter © 2012 Elsevier B.V. All rights reserved.
http://dx.doi.org/10.1016/j.bios.2012.09.036

its application range with emphasis on achieving usable sensitivity and reliability when the target analytes are at low concentration. AC electrokinetic phenomena, especially DEP, provide a means of in-situ concentration bioparticles/molecules to enhance the detection sensitivity as well as the selectivity of microelectrodes.

In the presence of an inhomogeneous electric field, DEP can manipulate particles based on the difference between the particle polarizability and that of the medium solution (Morgan et al., 1999). The induced DEP force is proportional to the square of the electric field strength gradient and the polarizability of the particle, the latter of which strongly depends on several factors, such as AC frequency range, buffer conditions and particle's dielectric properties. While there are many reports on DEP of DNA, most of them were done in deionized (DI) water or highly diluted DNA buffer (Henning et al., 2010). This research is among the first to work with DNA in practical buffer, such as physiological strength phosphate buffered saline (with 154 mM Na+, denoted as 1 × PBS from this point on), which is contrasted with most of previously reported DEP tests of DNA that were done in deionized water or highly diluted DNA buffer at merely 12.5 mM NaCl (Asbury et al., 2002) or 10 mM phosphate solution (Bakewell and Morgan, 2006; Regtmeier et al., 2007).

We have recently developed an AC electrokinetics (ACEK) enhanced impedance sensing technology that is capable of detecting bounded biomolecules in about two minutes, and this ACEK impedimetric method was employed here to characterize the DEP responses of two types of DNA of different and representative molecular conformations, including pUC18 in a supercoiled form and λDNA in a linear form. In our prior work, we have demonstrated ACEK concentration of biomolecules by both numerical study (Yang and Wu, 2010) and experiments (Liu et al., 2011), in which the deposition of biomolecules on the microchannel bottom was significantly accelerated by applying an appropriate AC signal over the interdigitated microelectrodes. This work is an improvement or simplification over the previous work, since impediment sensing does not need secondary fluorescent label and optical interface. This work employed simultaneous dielectrophoretic concentration and capacitive detection for characterization of DNA. Interdigitated microelectrode arrays were used to induce DEP response of the target DNAs, causing the attraction or repulsion of DNAs. In the meanwhile, the same set of microelectrode array was interrogated to detect the DNA deposition on the electrodes, so that the deposition process and the corresponding changes in the electrode impedance could be monitored in real time. We used this method to study the DEP impedimetric response of pUC18 and λ DNA. The results were validated using fluorescent labeled DNA through observation under a microscope. Since impedimetric sensing is a label-free technique, possible modification of DNA's dielectric properties by fluorescent dyes was also studied and discussed in this paper. The work presented here could yield very useful information for DEP characterization of DNA in a real-world setting, i.e. without fluorescent labeling and within an environment of physiological ion strength.

2. AC electrokinetics and impedance sensing

Recent advances in ACEK have shown its potential in the nanoscale manipulation of DNA. Comparing with DCEK, which is the underlying principle for gel-electrophoresis and capillary-electrophoresis, AC DEP has several advantages for DNA manipulation (Hughes, 2000; Wu, 2008): (1) suppressed electrochemical reactions because of time-varying AC electric current; (2) low voltages since AC DEP uses microelectrodes placed closely to each other in microchannels; (3) much reduced Joule heating since AC electric field exists locally where DEP force is needed.

In recent years, with the emergence of ACEK, efforts have been made to integrating ACEK concentration and impedance sensing (Wu et al., 2005a) to increase the sensitivity of impedance sensing. The purpose of integrating ACEK with impedance sensing is to use ACEK effects such as DEP to attract the particle within a short range to the microelectrode surface (comparable to characteristic length of the electrode array) so as to enhance the impedance response (Wu et al., 2005b). The presence of dielectric particles will alter the impedance of the electrode-liquid interface, thus producing a detectable impedance change.

When influenced by DEP and other ACEK effects, DNA molecules within that range can be attracted to or repelled from the electrodes, causing an impedance change corresponding to that particular AC condition and yielding their dielectric information. In general, DEP force on a spherical or rod-like particle can be expressed respectively as (Morgan and Green, 1997)

$$F_{\mathrm{DEP,\ sphere}} = 2\pi\varepsilon_{\mathrm{m}}R^3\mathrm{Re}\left[\frac{\varepsilon_{\mathrm{p}}^*-\varepsilon_{\mathrm{m}}^*}{\varepsilon_p^*+2\varepsilon_{\mathrm{m}}^*}\right]\nabla|E_{\mathrm{rms}}|^2, \tag{1}$$

and

$$F_{\mathrm{DEP,\ rod}} = \frac{\pi\varepsilon_{\mathrm{m}}lr^2}{3}\mathrm{Re}\left[\frac{\varepsilon_{\mathrm{p}}^*-\varepsilon_{\mathrm{m}}^*}{\varepsilon_{\mathrm{m}}^*}\right]\nabla|E_{\mathrm{rms}}|^2 \tag{2}$$

where ε_m is the dielectric constant of medium, R is the spherical particle diameter, l is the linear DNA length and r is the radius of its cross section. $\varepsilon_{\mathrm{p}}^*$, $\varepsilon_{\mathrm{m}}^*$ are the complex permittivities of the particle and the suspending medium, which are related to material permittivity ε and conductivity σ by $\varepsilon^*=\varepsilon+i\sigma/\omega$. So in an inhomogeneous electric field, when the particle is more polarizable than the suspending medium (i.e. $\varepsilon_{\mathrm{p}}^*-\varepsilon_{\mathrm{m}}^*>0$), particles will be attracted to the high field regions (e.g. electrode edges), known as positive DEP (p-DEP). A particle with lower polarizability than the suspending medium (i.e. $\varepsilon_{\mathrm{p}}^*-\varepsilon_{\mathrm{m}}^*<0$), will be repelled from the high field regions, known as negative DEP (n-DEP).

There are prior reports on using DEP techniques to probe the electrical properties of cells and bacteria and their responses to the electric field. By the same principle, it should be possible to use DEP to manipulate DNA as well. However, as it can be seen from Eq. (1), the magnitude of DEP force depends on the particle volume. In case of small DNA molecules such as pUC18 (2686 base pairs), DEP may not be effective unless the molecules are located within a very short distance to the electrodes (e.g. 1 μm). This problem could be alleviated by appropriate choices of electrode designs and electric signals. AC electric field in an electrolyte, when applied with properly designed electrodes, can induce fluid movements to carry target molecules to the electrodes for detection. At ionic strength of interest to this work, microflows are generated by AC electrothermal (ACET) effect. Previous study showed that ACET effect plays an important role in increasing detection sensitivity (Feldman et al., 2007; Liu et al., 2011). Because fluidic forces have no dependence on particle size, ACET microflows will be well suited for transporting small particles. Therefore, with appropriate electrode designs, inducing ACET microflows as an accompanying effect to DEP will be especially beneficial in the detection of small particles.

ACET effect arises from the uneven Joule heating of the fluid (Kheterpal and Mathies, 1999; Wu et al., 2007), which generates thermal gradients ∇T, consequently introducing inhomogeneities in conductivities and permittivities as $\nabla\varepsilon=(\partial\varepsilon/\partial T)\nabla T$ and $\nabla\sigma=(\partial\sigma/\partial T)\nabla T$. In turn, $\nabla\sigma$ and $\nabla\varepsilon$ generate mobile electric charges, ρ_E, in the fluid bulk, by $\rho_E=\nabla\cdot(\varepsilon\mathbf{E})=\nabla\varepsilon\cdot\mathbf{E}+\varepsilon\nabla\cdot\mathbf{E}$ and $(\partial\rho_E/\partial t)+\nabla\cdot(\sigma\mathbf{E})=0$ with $\partial/\partial t=i\omega$ in AC fields, where ω is

angular frequency. Through the induced charges, AC fields exert body forces on incompressible fluids as $\mathbf{f}_E = \rho\mathbf{E}$. Its time average is

$$\langle \mathbf{f}_{ACET} \rangle = -\frac{1}{2} K_{et}(\omega) \cdot \nabla T \cdot \varepsilon \mathbf{E}_0^2, \quad (3)$$

where $K_{et}(\omega) = (((\partial\sigma/\partial T)/\sigma) - ((\partial\varepsilon/\partial T)/\varepsilon))(1/(1+\omega^2\tau^2))$, and $\tau = \varepsilon/\sigma$ is electrolyte charge relaxation time. In an aqueous system, $1/\varepsilon(\partial\varepsilon/\partial T) = -0.4\%/\mathrm{K}$, $1/\sigma(\partial\sigma/\partial T) = 2\%/\mathrm{K}$, so $k_{et}(\omega) = 0.022/\mathrm{K}$ for AC frequency $\omega << 1/\tau$, leading to $\langle \mathbf{f}_{ACET} \rangle = -0.011 \cdot \nabla T \cdot \varepsilon \mathbf{E}_0^2$. With planar electrodes, prior work found that ACET effect will induce vortices above each electrode, and the microflows will convect the embedded particles towards the electrode surface (Lian et al., 2007).

The particle movement caused by ACET effect is additive to that by DEP. As ACET flows are induced by the energy dissipation in the fluid simply as $\langle P \rangle = \sigma E_{\mathrm{rms}}^2$, ACET effect does not have any frequency dependence. Therefore, the frequency dependence exhibited in particle movement is mostly caused by DEP, and can still be used to extract the DNA's dielectric properties.

In this work, AC signal applied over the microelectrodes will not only assist with the focusing of DNA onto the electrodes, but also be used to monitor the deposition process in real time, i.e. impedimetric sensing. Electrical impedance measurement has a long history of being used to characterize the electric properties of electrodes and surrounding liquid and to study the electron transfer kinetics at the interface of electrodes and liquid (Asbury et al., 2002). The impedance between a pair of electrodes immersed in liquid can be approximated as a series connection of the interfacial capacitor and resistive components including charge transfer resistance and electrolyte resistance. When the electrodes are immersed into a liquid electrolyte, a thin layer of counter ions is formed at the interface of the electrode and the fluid to neutralize the surface charges at the electrode, which is commonly known as electric double layer (EDL). The layer of counter ions and electrode surface charges is equivalent to the two plates in a capacitor with a separation distance of Debye length, which is determined by fluid conductivity (Castellanos et al., 2003). When macromolecules are adsorbed on the electrode surface, the electrode/electrolyte interfacial capacitance will change, which can be correlated to the deposition of macromolecules or particles on the electrode as well as the macromolecule/particle concentration in the fluid.

As schematically shown in Fig. 1, without any surface deposition, the bare electrode surface will yield interfacial capacitance with a thickness of Debye length and the interfacial capacitance can be expressed as, $C_0 = \varepsilon A/\lambda_d$, where C_0 is the original interfacial capacitance, ε is the dielectric constant of the EDL, A is the active area and λ_d is the thickness of the EDL, i.e. Debye length. When particles are deposited on the electrode surface, the thickness of the dielectric layer becomes the sum of the Debye length, λ_d and twice of the radius of the bounded particles, R. The interfacial capacitance then becomes $C = \varepsilon A/(2R+\lambda_d)$. Consequently, the surface binding can be detected through the relative change in interfacial capacitance. Because the dielectric properties of the DNA will determine the strength of DEP attraction it feels, further affecting the amount of DNAs to be deposited at the electrode surface and the relative change of interfacial capacitance at a given AC condition, the DEP response of DNAs can therefore be obtained from impedance readings.

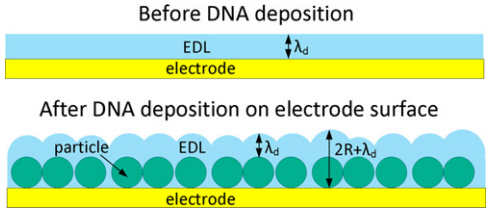

Fig. 1. Mechanism of capacitive sensing to detect the deposition of biomolecules at electrode surface.

3. Devices and methods

3.1. Microelectrode arrays

Commercial surface acoustic wave (SAW) resonator chips (PARS 433.92, AVX Corp) were used for ACEK manipulation and impedimetric measurements of DNA samples. Similar types of SAW chips have been used by other groups (Stanke et al., 2011) to study ACEK effects, and fluid streaming above the electrodes has been observed in DEP experiments from 10 Hz to 1 GHz, which supports our discussion on the role of ACET effect in the previous section.

Before use, the top of the metal casing around the SAW resonator was opened mechanically to expose the working electrode array inside. The interdigitated electrodes are made of aluminum deposited on quartz substrate, with the dimensions of 1.4 μm width and 1.1 μm spacing between the electrodes. A photograph of the opened SAW chip and a scanning electron micrograph of the interdigitated electrodes are given in Fig. 1 in the supplementary material section. The interdigitated electrodes are electrically connected to two contact pads on the chip bottom, which are then connected to an impedance analyzer. Our experiments use a frequency range up to 5 MHz, which is much lower than the SAW chip's resonant frequency of 433.92 MHz. So the interdigitated electrode array in our experiments is merely a means to apply desired AC electric field onto the sample solutions. The metal casing around the electrode chip is about 4 mm (L) × 2.5 mm (W) × 1 mm (H) = 10 μL, serving as a microchamber for sample solutions.

The electrodes were prepared for experiments as follows. Firstly, the opened SAW chips were washed with acetone, isopropyl alcohol, and DI water sequentially, to remove possible organic contamination. Then, they were plasma-treated for 30 s at 50 W to render the chip surface hydrophilic. Afterwards, a 5 μL sample solution was loaded into the metal casing around the electrode chip.

3.2. Equivalent circuit of microelectrode/fluid system

For intermediate frequency range as used in this work (kHz to MHz), the impedimetric behavior of interdigitated microelectrodes in aqueous solutions is commonly represented by an equivalent circuit shown as the inset in Fig. 2 (Yang, 2008; Sabounchi et al., 2008). In the equivalent circuit, C_{dl} accounts for the interfacial capacitance between the electrolyte and electrodes, R_{s} is the resistance of the solution between the two electrodes, and C_{s} is the dielectric capacitance of the solution. There are two paths for electric currents. The electric fields could go through the electrode/electrolyte interfaces and then through the electrolyte bulk, represented by two identical capacitors C_{dl} in series with a resistor R_{s}, or could be coupled between the microelectrodes with the electrolyte as the dielectric medium, as represented by a capacitor C_{s} in Fig. 2.

To understand the impedance property of the SAW microelectrodes, the impedance spectrum of the microelectrodes was obtained from 5 kHz to 110 MHz, which is the frequency range of interest for this work. The data were acquired using a precision impedance analyzer (Agilent® 4294 A) and transmitted to a computer through its LAN port. The measurement was conducted with 5 mVrms of excitation voltage using physiological strength PBS. Fig. 2 shows its Bode plot, along with two curve fitting

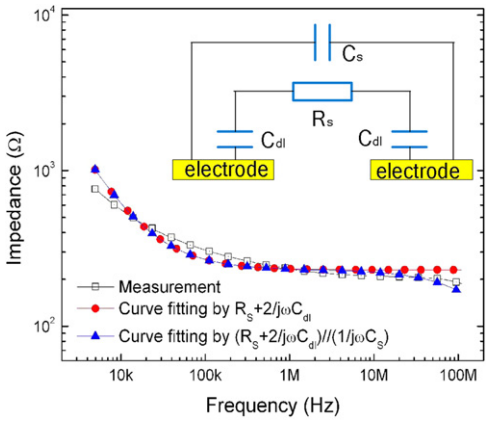

Fig. 2. Impedance spectrum of SAW microelectrodes (open square), and its comparison with two curve fittings by R_s-C_{dl} series connection (solid circle) and by the whole equivalent circuit in the inset (solid triangle).

results. One fitted curve was done using the whole equivalent circuit in Fig. 2 and the other was done using only the lower R_s-C_{dl} path (i.e. neglecting C_s). The circuit components are extracted to be $C_{dl}=82$ nF. $R_s=230\,\Omega$, and $C_s=2.5$ pF. It can be seen that both fitted curves showed reasonably good agreements with the measured results. At frequencies above 20 MHz, the curve fitting by the whole circuit goes down slightly with frequency, closely following the measured data, whereas the fitted curve using R_s-C_{dl} path only showed constant impedance at high frequencies. The difference is caused by the dielectric shunting from C_s ($1/\omega C_s$, $\omega=2\pi f$ is angular frequency) at high frequencies. Below 20 MHz, $1/\omega C_s$ poses a much higher impedance than that by R_s-C_{dl} in series (i.e. $\sqrt{R_S^2+(1/\omega C_{dl})^2}$). Even at 20 MHz, $1/\omega C_s$ still presents an impedance of 3.18 kΩ, in contrast to a mere 232 Ω by the R_s-C_{dl} path. The above analysis shows that for the frequency range of interest to this work (20 kHz to 5 MHz), a serial connection of R_s and C_{dl} could be used to simulate the impedance presented by the microelectrode/fluid system.

3.3. DEP impedance measurement methods

During DEP impedance measurements, the impedance data were continuously recorded at fixed excitation frequencies and an elevated voltage level of 500 mV_{rms} for 5 min, which is much higher than typically used 5 mV_{rms} in traditional impedance measurements. Such a voltage level is sufficient to induce ACEK effects at that frequency and provide us with information on the impedance change as a result of DNA deposition on the electrodes. The impedance data were acquired using a precision impedance analyzer (Agilent® 4294 A), and an oscilloscope (TDS2024, Tektronix, USA) was used to verify that specified voltages were applied on the electrodes in all tests.

The measured impedance, Z_{sens}, is in the form of $Z_{sens}=R-jX=R+1/j\omega C_{meas}$, where R and X are the real part and imaginary part of the measured impedance. From the imaginary part, a capacitance value of $C_{meas}=1/\omega X$ can be found for a preset angular frequency. Our study of the electrode impedance spectra in Section 3.2 showed that for the frequency range of interest to this work (20 kHz to 5 MHz), a serial connection of fluid resistance and interfacial capacitance could be used to simulate the impedance presented by the microelectrode/fluid system. Therefore, in this work, C_{meas} corresponds approximately to $C_{dl}/2$ in Section 3.2 (C_{meas} is two C_{dl} in series), and the change in C_{meas} is employed to correlate with the deposition on the electrode surface.

Further, to minimize the effect of capacitance inconsistence from one electrode array to another, normalized capacitance is used and calculated as $Norm(C_t)=C_{t,meas}/C_{0,\ meas}$, where $C_{t,meas}$ and $C_{0,\ meas}$ are the capacitance values at time t and time zero, respectively. The normalized capacitance change rate is employed to indicate the DNA deposition on electrode surfaces, which is the slope of normalized capacitance as a function of time and found by least square linear fitting method.

Control experiments using blank buffer solution were included to ensure that capacitance changes were not caused by possible electrochemical reactions. Even though a relatively high voltage level of 500 mV_{rms} was used on high ionic strength solutions, the impedance measurements were conducted at sufficiently high frequencies and the reactions were avoided. From 20 kHz to 5 MHz, the capacitance changes of blank PBS buffer under 500 mV_{rms} in 5 min were found to be less than $\pm 0.4\%$ for all conditions, and the capacitance changes appeared in an erratic manner, probably due to experimental uncertainties. In contrast, obvious capacitance changes were detected at higher voltage (e.g. 5 V_{rms}) or low frequency (e.g. 100 Hz) for blank samples. Based on the results from control experiments, capacitance changes due to possible electrochemical reaction is negligible.

4. Results and discussion

In this section, DEP characterization of DNA and fluorophore were performed using two methods, including fluorescent imaging and impedimetric measurement. Fluorescent imaging with labeled molecules is well established for qualitative characterization of particles' dielectric properties. A good correlation between fluorescent imaging results and impedance measurement data serves to validate the impedimetric method presented here. Then the impedimetric method can be used to study the DEP properties of unlabeled DNAs and fluorophores.

4.1. DEP characterization by fluorescent imaging

The first set of our experiments is to find out the DEP response of DNA using fluorescence imaging. Both types of DNAs (pUC18 and λDNA) were labeled with fluorescent dye SYBR Gold nucleic acid gel stain (Invitrogen, Ltd.), with excitation and emission wavelengths at 494 nm and 537 nm, respectively. A fluorescence microscope (NIKON eclipse lv-100, Japan) equipped with a CCD camera (Photometrics CoolSNAP ES, Roper Scientific, Germany) and a fluorescence illumination system (X-Cite® 120, EXFO Photonic Solutions Inc., Canada) was used to observe and evaluate the fluorescence density.

For DEP characterization by fluorescence imaging, we used a set of four gold polynomial microelectrodes deposited on silicon wafer. The quad polynomial electrode design has been widely adopted for DEP characterization (Green et al., 2000), since it will show both positive and negative DEP clearly (Huang and Pethig, 1991). Because DEP response is dependent on electric field gradient and frequency rather than any particular electrode design, DEP responses obtained with quad electrodes can be readily applied to the interdigitated sensing electrodes.

DEP characterization of fluorescently labeled DNA was conducted at different AC frequencies of 20 kHz, 50 kHz, 100 kHz, 300 kHz, 500 kHz, 1 MHz, 2 MHz, and 5 MHz, respectively. The spacing between the adjacent electrodes was 10 μm. So an AC voltage of 10 Vpp was applied to obtain a comparable level of electric field with that in interdigitated sensing electrodes. Fluorescence images were captured before and after applying AC voltages, and DEP response can be identified by comparing the grey scale value of fluorescence images. pUC18 experienced

strong positive DEP at 300 kHz and exhibited obvious negative DEP at 5 MHz. For λ DNA, positive DEP was found to be most pronounced at 100 kHz, and obvious negative DEP was observed above 2 MHz. Fig. 2(a) and (b) in the supplementary material section showed two representative micrographs of DNA undergoing positive and negative DEP, respectively, in which115.5 nM pUC18 DNA in 1 × PBS solution (154 mM Na+) was used.

4.2. DEP responses of DNA and fluorophore by impedance measurement

Subsequently, we performed DEP characterization of DNA using ACEK enhanced impedance measurement at frequencies corresponding to those used in the fluorescent imaging. To determine the effect of fluorescence label on the DEP response of DNA, we also conducted ACEK based impedimetric study of unlabeled pUC18. Capacitance change rates of pUC18, both labeled and unlabeled, are given in Fig. 3 at frequencies from 20 kHz to 5 MHz. At first, the absolute capacitance change monotonously increases with frequency from ~1% per minute (indicating very weak *p*-DEP) at 20 kHz to ~5% per minute at 300–500 kHz, then it decreases from its peak value to 0.5% per minute at 5 MHz. The highest capacitance change of ~−5% per minute occurs at 300 kHz for labeled pUC18 and 500 kHz for unlabeled pUC18. The none-to-little change in capacitance indicates negative DEP for the tested frequency range. The impedance results of labeled pUC18 in Fig. 3 are consistent with our observation from fluorescence imaging. Control experiment using only 1 × PBS was also included (open circle in Fig. 3), which shows very little change for all test frequencies. The results support that the DEP response can be obtained by impedance measurement.

An important feature of impedimetric sensing is that it is a label-free detection technique. So far, all the work performed on DEP characterization of DNA adopted fluorescence labeled DNA. The addition of fluorescence label may alter the DEP response of unlabeled DNAs, and in the case of small DNA molecules the DEP response from the fluorescence label may dominate over that of DNA, which could adversely affect DEP separation of small DNA molecules.

Comparison of capacitance data for labeled and unlabeled pUC18 showed that at low frequencies from 20 kHz to 100 kHz and at high frequencies above 2 MHz, there is no appreciable difference between labeled and unlabeled DNA in the magnitude of capacitance change. There is a slight offset in AC frequency when the *p*-DEP forces for labeled and unlabeled pUC18 reach their maxima. At 500 kHz, unlabeled pUC18 exhibits much stronger *p*-DEP than labeled pUC18, while at 300 kHz labeled pUC18 experiences slightly stronger *p*-DEP than unlabeled one. Meanwhile, 1 × PBS buffer solution dispersed with SYBR Gold was also tested as control, and its capacitance changes were close to zero for all frequencies. We can tentatively conclude that fluorescent dye has limited effect on the DNA's DEP frequency response. It does not change the polarity of DEP force, but could possibly affect DEP force magnitude and peak frequency by a small amount.

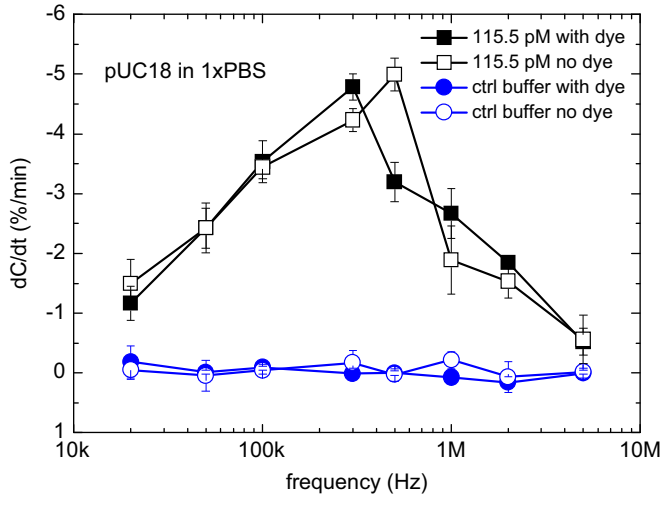

Fig. 3. DEP response of pUC18 in 1 × PBS obtained using ACEK enhanced impedance measurement. Both fluorescence labeled and unlabeled pUC18 were tested along with control samples.

4.3. Effects of DNA concentrations

Next experiment studied whether DNA concentration will cause any changes in its DEP response. Lower concentrations of unlabeled pUC18 from 57.8 pM to 2.89 pM were obtained by diluting 115.5 pM pUC18 with 1 × PBS. The results of four dilutions of unlabeled pUC18, 115.5 pM, 57.8 pM, 28.9 pM and 5.78 pM, are shown in Fig. 4. As DNA becomes more diluted, the capacitance change decreases accordingly, indicating that this method is capable of quantitative detection of macromolecules. For lower pUC18 concentrations from 57.8 pM to 5.78 pM, the largest capacitance change rates occur at 300 kHz, which shifts from the 500 kHz peak at 115.5 pM. In Fig. 4, the lowest detectable concentration is 5.78 pM. At 2.89 pM (data not shown),

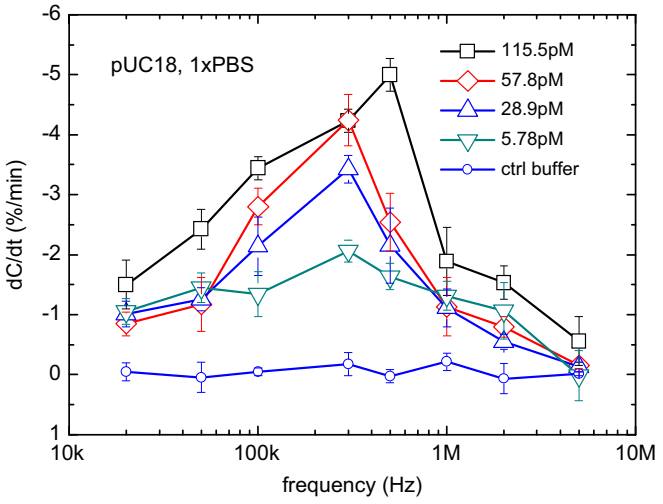

Fig. 4. Capacitance change rates of unlabeled pUC18 at different concentrations.

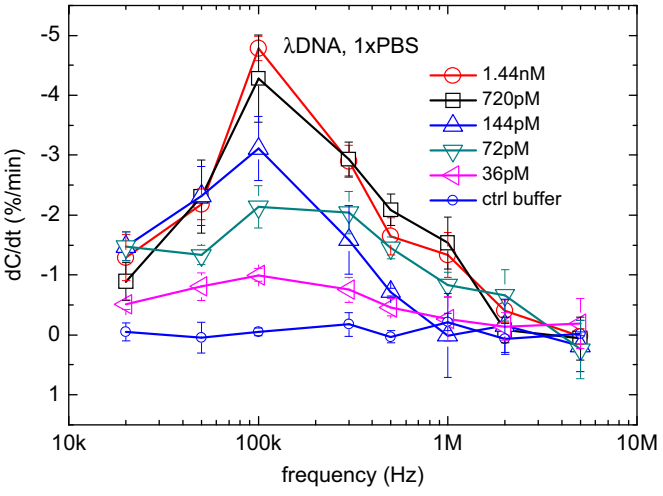

Fig. 5. Capacitance change rate of unlabeled λ DNA in 1 × PBS.

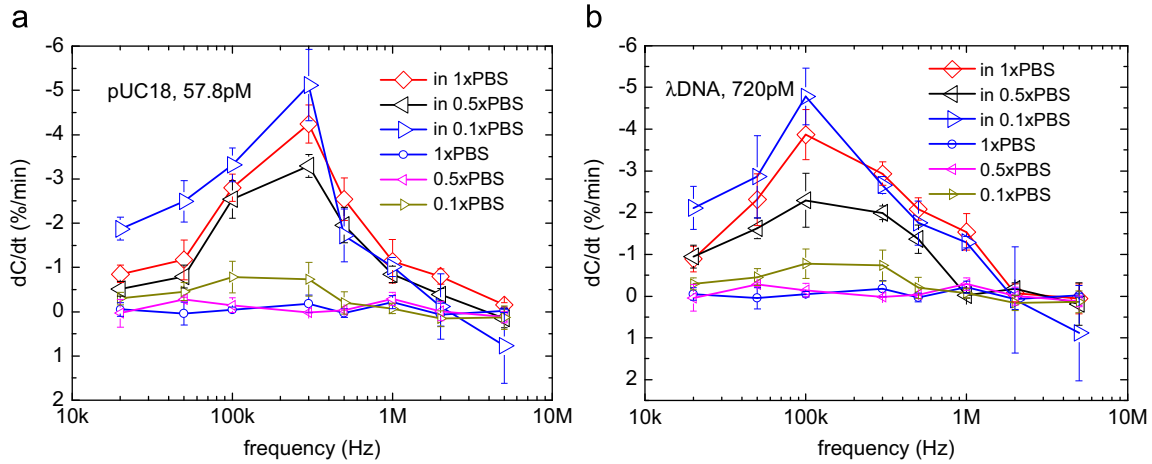

Fig. 6. Capacitance change rate of unlabled DNA in diluted PBS. (a) Capacitance change of pUC18 in diluted PBS (b) capacitance change of λ DNA in diluted PBS.

the capacitance change cannot be differentiated from that of control solution. So 5–6 pM may very well be the lower detection limit of this method.

DEP response of unlabeled linear λ DNA was also studied, and the results are shown in Fig. 5. Higher concentration of λDNA than pUC18 were used here, 1.44 nM versus 115.5 pM. When λ DNA concentration goes from 0.72 nM down to 14.7 pM, the capacitance change rate decreases accordingly. The DEP responses are very close between 1.44 nM and 0.72 nM. It seems that DNA concentration in the nM range will not affect its DEP response, which is probably caused by saturation of electrode surface at high λ DNA concentration. Overall, it appears that different concentrations of λ DNA affects only the magnitude of capacitance change, not the frequency dependence. It can also be noticed from the measurement results shown in Fig. 5 that the largest capacitance change of $\sim -4.4\%$ from 720 nM λDNA is about the same level as that produced by 115.5 nM pUC18, while more than 5 times of λDNA were used here. According to Eqs. (1) and (2), linear DNA will experience much weaker DEP force than spherical DNA, even though λDNA has a higher molecular weight than pUC18. This confirms that DEP response of linear DNA will be much weaker than supercoiled DNA. The DEP responses for 36 pM linear λ DNA are very weak, can hardly be differentiated from that of control solution. It appears that linear λ DNA has a limit of detection around 72 pM.

The frequency response of λDNA is also different from that of supercoiled pUC18. The positive DEP is consistently shown to be most pronounced at 100 kHz for all the concentrations tested. In contrast, pUC18 has positive DEP around 300 kHz to 500 kHz. λDNA experiences *n*-DEP above 2 MHz, and *n*-DEP for pUC18 is at 5 MHz. Therefore it is plausible that DNAs of different molecular conformations can be effectively separated based on their DEP responses by applying ac electrical voltages within the appropriate frequency range.

4.4. Effects of buffer ionic concentration

It is well known that DEP response depends on the properties of suspending medium. Fig. 5 shows DEP frequency dependence of 57.8 pM pUC18 and 720 pM λ DNA in $1\times$, $0.5\times$ and $0.1\times$ PBS. For pUC18, as shown in Fig. 6(a), the DEP response for DNA in $0.5\times$ and $0.1\times$ PBS were similar to that in $1\times$ PBS. The responses at all frequencies followed similar contours, with peak values at 300 kHz. The sample in $0.1\times$ PBS consistently yielded the highest response among the three buffers, which can be explained with the term of $(\varepsilon_p^*-\varepsilon_m^*)$ in Eq. (1). Because complex permittivity ε^* is proportional to material conductivity, *p*-DEP is stronger with less conductive medium. Lower capacitance change rate is observed for $0.5\times$ PBS sample, which is probably due to reduced ACET flows arising from a lower electric conductivity of the sample solution. Capacitance changes for $1\times$, $0.5\times$ and $0.1\times$ PBS control buffers were negligible, as expected.

The capacitance changes for λ DNA in $1\times$, $0.5\times$ and $0.1\times$ PBS are given in Fig. 6(b). The λ DNA concentration used here is 0.72 nM. With varying buffer concentration, the DEP responses of linear λDNA show very similar trends to those of pUC18. Impedance responses become weaker when the buffer concentration changes from $1\times$ PBS to $0.5\times$ PBS. No obvious positive DEP is detected for linear λ DNA at $0.5\times$ PBS was used. Besides the weaker ACET flows at $0.5\times$ PBS, one probable cause is that the (di)electric characteristics of λ DNA and $0.5\times$ PBS are very close under this condition. At $0.1\times$ PBS, stronger DEP responses were observed for linear λ DNA as well, probably due to the same reason.

5. Conclusion

Characterization of the DNA's DEP behavior is the foundation of manipulating DNA by electric fields. This work reported an ACEK enhanced impedimetric technique that has potential for real time detection of macromolecules in physiological solutions. Furthermore, using this method, we have investigated the feasibility of electric characterization of DNA based on the prominent DEP dependence of DNA on their conformations and types. Our experimental results reported in this paper support the validity of ACEK impedance measurements. The work here can provide the basis for particle separation, disease diagnose, cell life circle research in physiological surroundings.

Acknowledgement

This study was supported by the U.S. National Science Foundation under Grant No. ECS-0448896, and China's Natural Science Foundation under Grant No. 51075087. Micro fabrication of this research was conducted at the Center for Nanophase Materials Sciences, which is sponsored at Oak Ridge National Laboratory by the Scientific User Facilities Division, U.S. Department of Energy. S. Li gratefully acknowledge the financial support from China Scholarship Council (No.2010612182).

Appendix A. Supporting information

Supplementary data associated with this article can be found in the online version at http://dx.doi.org/10.1016/j.bios.2012.09.036.

References

Asbury, C.L., Diercks, A.H., van den Engh, G., 2002. Electrophoresis 23 (16), 2658–2666.
Bakewell, D.J., Morgan, H., 2006. IEEE Transactions on NanoBioscience 5 (2), 139–146.
Castellanos, A., Ramos, A., Gonzalez, A., Green, N.G., Morgan, H., 2003. Journal of Physics D: Applied Physics 36, 2584.
Feldman, H.C., Sigurdson, M., Meinhart, C.D., 2007. Lab on a Chip 7 (11), 1553–1559.
Green, N.G., Ramos, A., Morgan, H., 2000. Journal of Physics D: Applied Physics 33, 632.
Henning, A., Bier, F.F., Ralph, H., 2010. Biomicrofluidics 4, 022803.
Huang, Y., Pethig, R., 1991. Measurement Science and Technology 2, 1142.
Hughes, M.P., 2000. Nanotechnology 11, 124.
Kheterpal, I., Mathies, R.A., 1999. Analytical Chemistry 71 (1), 31–37.
Lian, M., Islam, N., Wu, J., 2007. IET Nanobiotechnology 1 (3), 36–43.
Liu, X., Yang, K., Wadhwa, A., Eda, S., Li, S., Wu, J., 2011. Sensors and Actuators A: Physical 171 (2), 406–413.
Lorenz, W., Schulze, K.D., 1975. Journal of Electro Analytical Chemistry 65 (1), 12.
Morgan, H., Green, N.G., 1997. Journal of Electrostatics 42 (3), 279–293.
Morgan, H., Hughes, M.P., Green, N.G., 1999. Biophysical Journal 77 (1), 516–525.
Regtmeier, J., Duong, T.T., Eichhorn, R., Anselmetti, D., Ros, A., 2007. Analytical Chemistry 79 (10), 3925–3932.
Sabounchi, P., Morales, A.M., Ponce, P., Lee, L.P., Simmons, B.A., Davalos, R.V., 2008. Biomedical Microdevices 10, 661–670.
Stanke, S., Bier, F.F., Heelzel, R., 2011. Electrophoresis 32, 2448–2455.
Wang, M., Wang, L., Wang, G., Ji, X., Bai, Y., Li, T., Gong, S., Li, J., 2004. Biosensors and Bioelectronics 19 (6), 575–582.
Wu, J., 2008. IET Nanobiotechnology 2 (1), 14–27.
Wu, J., Ben, Y., Chang, H.C., 2005a. Industrial and Engineering Chemistry Research 44 (8), 2815–2822.
Wu, J., Ben, Y., Chang, H.C., 2005b. Microfluidics and Nanofluidics 1 (2), 161–167.
Wu, J., Lian, M., Yang, K., 2007. Applied Physics Letters 90 (23) 234103-234103-234103.
Yang, K., Wu, J., 2010. Biomicrofluidics 4, 034106.
Yang, L., 2008. Talanta 74 (5), 1621–1629.